

X-RAY COMPUTED TOMOGRAPHIC RECONSTRUCTION AND BONE HISTOLOGY OF  
THE AETOSAUR *COAHOMASUCHUS CHATHAMENSIS* (ARCHOSAURIA:  
STAGONOLEPIDIDAE) FROM THE UPPER TRIASSIC PEKIN FORMATION, DEEP RIVER  
BASIN, NORTH CAROLINA AND A RE-ANALYSIS OF ITS PHYLOGENETIC  
RELATIONSHIPS

by

Devin Kane Fodor Hoffman

Honors Thesis

Appalachian State University

Submitted to the Department of Geology  
and The Honors College  
in partial fulfillment of the requirements for the degree of

Bachelor of Science

May, 2017

Approved by:

---

Andrew B. Heckert, Ph.D., Thesis Director

---

Michael S. Osbourn, Ph.D., Second Reader

---

Gabriele M. Casale, Ph.D., Departmental Honors Director

---

Ted Zerucha, Ph.D., Interim Director, The Honors College

## ABSTRACT

Aetosauria is a clade of heavily armored, quadrupedal archosaurian omnivores to herbivores known from Upper Triassic units from across what was the supercontinent of Pangea. Their relative abundance in many deposits, as well as the sparsity of other Triassic herbivores, indicates they were key components of Late Triassic ecosystems. However, there remains debate about the relationships within the clade, the structure of their internal skeletal anatomy, and their patterns of growth. To contribute answers to these questions I reexamined and reanalyzed a recently described species of *Coahomasuchus* from the Sanford sub-basin of North Carolina, *C. chathamensis*. My phylogenetic analysis, with updated character scorings for *Coahomasuchus* and several other aetosaurs, recovers *Coahomasuchus* in a polytomy with *Aetosaurus* and the Typothoracinae, in contrast with a recent analysis that recovered *Coahomasuchus* as highly labile. In an attempt to better understand the interior skeleton of an aetosaur, I undertook the first CT reconstruction of the skeleton under the armor of an articulated specimen. These scans revealed several previously unseen elements, including several articulated vertebrae and ribs, an isolated vertebra, left ulna, and the right humerus. To better characterize growth in the clade, I undertook a histological examination of *C. chathamensis*, sampling a paramedian osteoderm from the holotype as well as five osteoderms (two paramedian, one lateral, and two of uncertain position) and two incomplete limb bones (tibia and fibula) from referred specimens discovered at the holotype locality. From these sections I estimated specimen ages by using lines of arrested growth (LAGs) to determine that the sampled individuals ranged from two to eight years old. When compared to similarly sized aetosaurs, it can be inferred *C. chathamensis* was growing relatively rapidly. The discovery reveals that the holotype of *C. chathamensis* is apparently a juvenile individual.

## ACKNOWLEDGEMENTS

Support for this research came from the Appalachian State University Office of Student Research and the Department of Geology. I would like to thank the following people for their contributions to my research: My committee, Dr. Andy Heckert and Dr. Michael Osbourn for research and writing guidance, Anthony Love and Lisa Herzog for teaching me histological techniques, Yanelis Delgado for assisting me with histologic sectioning, Jason Bourke for his help with CT scanning and Avizo advice, Lindsay Zanno for access to equipment and facilities, Siemens Medical Training Facility and NCSU College of Veterinary Medicine for the use of CT equipment, Vince Schneider and Trish Weaver for access and assistance in collections, and the North Carolina Museum of Natural Sciences for loaning specimens for my studies. Additionally, I would like to thank Dr. Heckert for his constant support and advice throughout my four years at Appalachian State University, and for my friends' and family's moral support during the writing of this thesis.

## TABLE OF CONTENTS

Abstract.....	2
Acknowledgements.....	3
Introduction.....	5
Geologic Setting.....	7
Phylogenetic Analysis.....	9
CT Reconstruction.....	12
Histology.....	14
Literature Cited.....	21
Tables.....	28
Figures.....	31

Abbreviations – North Carolina Museum of Natural Sciences (NCSM), North Carolina State University (NCSU)

## INTRODUCTION

The aetosaurs comprise a clade of heavily armored, quadrupedal herbivorous to faunivorous pseudosuchian-line archosaurs (Parker, 2016a; Heckert et al., 2017). Aetosaurs are known from Upper Triassic deposits from across Pangea, with fossil specimens known from every continent except Antarctica and Australia (Heckert and Lucas, 2000; Desojo et al., 2013; Schoch and Desojo, 2016; Heckert et al., 2017). They form a key component of Late Triassic ecosystems as one of the few lineages of non-dinosaurian archosauromorphs (along with rhynchosaurs) to have evolved herbivory during the Triassic (Desojo et al., 2013; Heckert et al., 2017). Therefore, understanding aetosaur phylogenetic relationships, skeletal anatomy, and ontogenetic growth patterns are important for building the bigger picture of archosaur diversification during the Triassic.

However, all three of these goals have their own inherent challenges to them. Aetosaur phylogenetic analyses are complicated by the presence of hundreds of osteoderms, often found dissociated from each other, as well as the rest of the skeleton, which have been used as the basis of character scorings for this group (Heckert and Lucas, 1999, 2000; Desojo et al. 2013; Parker, 2016a). Because of this armor, the internal skeletal anatomy of many species is poorly understood, as the best preserved aetosaur specimens are articulated, and thus the osteoderms obscure much of the appendicular and axial skeleton including, sometimes, features of the osteoderms themselves. Additionally, some aetosaur taxa (e.g. *Gorgetosuchus*) are known exclusively from osteoderms (Heckert et al., 2015), and are thus difficult to incorporate into phylogenetic analyses. A largely articulated presacral skeleton of the recently described species *Coahomasuchus chathamensis* (NCSM 23618) from the Upper Triassic of North Carolina (Figure 1) allowed for additional scorings of *Coahomasuchus* (Heckert et al., 2017) and the possibility of additional scoring through the use of X-ray computed tomography (CT). To date, no study has attempted to “remove” the osteoderm armor of an aetosaur using CT imaging, nor has this been attempted in other

armored fossil groups, though individual osteoderms of dinosaurs (e.g. Rodgers et al., 2011) and modern armored animals, such as armadillos and pangolins (e.g. Kawashima et al., 2015) have been imaged with CT technology.

*Coahomasuchus chathamensis* is the second species known from the genus *Coahomasuchus*, the first being *C. kahleorum* (Heckert and Lucas, 1999). Currently, *C. kahleorum* is known from one published specimen, the holotype skeleton, found near Coahoma, Texas in the Upper Triassic Carnian (Otischalkian) Colorado City Member of the Dockum Formation of the Chinle Group (Heckert and Lucas, 1999). The type specimen is a nearly complete, articulated skeleton approximately 71 cm long with complete osteoderm sets from the cervical to the middle of the tail, the braincase, parts of each limb and their respective girdles, appendicular osteoderms, and much of the vertebral column (Heckert and Lucas, 1999). Assuming it is an adult, *C. kahleorum* is relatively small bodied, and can be distinguished from co-occurring aetosaurs by its parallel, sub-radial ornamentation (Heckert and Lucas, 1999). In Heckert and Lucas' (1999) original analysis, *C. kahleorum* was found to be a relatively primitive aetosaur, and seen as filling the apparent stratigraphic gap or "ghost lineage" between late appearing primitive aetosaurs like *Aetosaurus* and early forms with derived characteristics such as *Desmatosuchus* and *Longosuchus* (Heckert and Lucas, 1999). There is also a second, undescribed specimen, located at the Texas Memorial Museum, Parker (2016a) used for some of the characters scored for *Coahomasuchus* in his phylogenetic analysis. The specimen remains under study by Parker and was not described as part of this study.

All fossil specimens of *C. chathamensis*, including the holotype specimen and referred materials from the holotype locality, are housed in the vertebrate paleontology collections at NCSM. All fossil preparation was performed at NCSM following the procedure described by Heckert et al. (2017).

Although Heckert et al. (2017) described some of the referred specimens, their list of specimens requires updating. After examining the NCSM collections, I was able to refer at least 27 additional specimens to *C. chathamensis* (Figure 1).

#### GEOLOGIC SETTING

The specimens of *C. chathamensis* come from NCSM locality NCPALEO1902, a brick quarry in Chatham County, North Carolina (Figure 1). This locality is in the Sanford sub-basin, part of the larger Newark Supergroup (Heckert et al., 2017). All of the Triassic sedimentary rocks in North Carolina were referred to the Chatham Group of the Newark Supergroup by Olsen (1997) and Weems and Olsen (1997). This assignment was based on the synchronous deposition of the units in rift basins during the break up of Pangea along nearly the entire eastern margin of North America (Weems and Olsen, 1997). The Sanford sub-basin represents a half-graben bounded by the Jonesboro fault system (normal faults) on the eastern margin (Olsen et al., 1991). This region contains three formations originally described by Campbell and Kimball (1923), in ascending order: the Pekin, Cumnock, and Sanford formations, all of which yield fossils (Figure 2). The upper and lower formations (Pekin and Sanford) are largely “red-bed,” sandstone-dominated units surrounding the Cumnock Formation of mostly gray claystone with occasional coal seams (Olsen et al., 1991; Heckert et al., 2017). Other fossils from this same locality include cynodonts (Lui and Sues, 2010), dicynodonts (Green et al., 2005; Green, 2012), the crocodylomorph *Carnufex carolinensis* (Zanno et al., 2015; Drymala and Zanno, 2016), aetosaurs, such as recently described *Gorgetosuchus* (Heckert et al., 2015), and numerous unpublished specimens.

All of the *C. chathamensis* material, and, indeed, essentially all of the vertebrate material was recovered from the uppermost portion of the Pekin Formation (Heckert et al., 2017). These fossils came primarily from a fine-grained red siltstone, and some osteoderms from a coarser-grained greywacke (Heckert et al., 2017), with many other fossils found in conglomerates and sandstones. The coarser lithologic units have been interpreted as fluvial

channels or as alluvial fan deposits (Olsen et al., 1991; Heckert et al., 2017). Determining the exact stratigraphic position of these specimens in the Pekin Formation is not possible due to the mining method of the brick quarry, and can be most specifically be assigned to the upper half of the formation (Heckert et al., 2017). This is because large (meter scale) blocks are removed from the main body of the quarry and left to weather on the quarry floor, as the brick operation is focused primarily on the surrounding layers of clay (Heckert et al., 2017). Fossils from these isolated blocks were identified by NCSM field crews, which then cut them out using a rock saw, before transporting them back to the NCSM for preparation (Heckert et al., 2017).

As the stratigraphically lowest unit in the Newark Supergroup locally, the Pekin has long attracted interest in its age. Palynostratigraphy has historically positioned the Pekin Formation in the Carnian stage (e.g. Cornet, 1993; Litwin and Ash, 1993), further verified by the vertebrate stratigraphic correlations made by Huber et al. (1993) and Lucas and Huber (2003). More recently, much of the Newark Supergroup thought to be Carnian in age has been reassigned to the Norian stage on the basis of the “long Norian,” with a Carnian–Norian boundary of ca. 228 Ma (Muttoni et al., 2004; Furin et al., 2006). Although the “long Norian” has been questioned (e.g. Lucas et al., 2012), the most recent age for the Pekin Formation comes from Whiteside et al. (2011), whose paleomagnetostratigraphic correlations with other Newark Supergroup units suggests an age of 231 Ma for the Pekin Formation. This age fits with both the “long Norian” (Muttoni et al., 2004; Furin et al., 2006) and Lucas’ (2010) Triassic timescales for the Carnian and makes *C. chathamensis* one of the oldest known aetosaurs as, to date, there are no pre-Carnian aetosaurs known (Heckert and Lucas, 2000; Desojo et al., 2013).

In the case of *Coahomasuchus*, the three most recent phylogenetic hypothesis (Heckert et al., 2015; Schoch and Desojo, 2016; Parker, 2016a) each posit a different hypothesis of the phylogenetic relationships of *Coahomasuchus* relative to other aetosaurs.

## PHYLOGENETIC ANALYSIS

**Methods** – The new species of *Coahomasuchus* allows for several new character scorings to be added to existing character matrices of aetosaurs. In their recent phylogenetic analysis Schoch and Desojo (2016) found *Coahomasuchus* to be a liable taxon within Aetosauria, but their analysis lacked several recent character changes of *Coahomasuchus* and other aetosaur taxa, including *Lucasuchus*, *Longosuchus*, and the recently described *Gorgetosuchus* (Heckert et al., 2015; Parker, 2016a). Therefore, a new analysis is required incorporating the updated characters and results from other studies (Heckert et al., 2015; Parker, 2016a), and the new character scorings for *C. chathamensis* (Heckert et al., 2017) to test if this result stays consistent. The data matrix I used was therefore updated from Schoch and Desojo (2016), itself based on the original matrix from Parker (2007). The matrix contains 24 taxa and 44 characters, with all the same taxa as Schoch and Desojo (2016), except for the addition of *Gorgetosuchus* (Heckert et al., 2015). I also incorporated all scoring updates from Heckert et al. (2015).

Cladistic analysis was performed using TNT 1.5 (Goloboff et al., 2008) following the procedure used by Schoch and Desojo (2016) to ensure as accurate a comparison as possible to see the effects of the updated scorings. Specifically, I performed a traditional search with 50 replications of Wagner trees (with random addition sequence), followed by the TBR branch swapping algorithm (holding 10 trees per replicate) (Schoch and Desojo, 2016). To ensure the use of TNT 1.5 rather than TNT 1.1 would not alter results, first I recreated the analysis from Schoch and Desojo (2016), exactly replicating the results of 9 most parsimonious trees (MPTs) of 95 steps and *Coahomasuchus* as the wild card (liable) taxon prior to running the updated analysis. Strict consensus trees were generated by collapsing zero length branches of the MPTs and all tree figures were generated using Adobe Illustrator.

**Results** – My new phylogenetic analysis with updated character scorings resulted in 4 MPTs, with a strict consensus tree of 100 steps (Figure 3). I recovered *Coahomasuchus* in a polytomy with *Aetosaurus* and Typothoracinae, in contrast with to Schoch and Desojo's (2016) result that found *Coahomasuchus* as highly labile (Schoch and Desojo, 2016). Additionally, I found *Lucasuchus* to be a wild card taxon, creating a polytomy within Desmotosuchinae, using TNT's Trees Comparison – Iter PCR function to identify *Lucasuchus* as the liable taxon function. After removing *Lucasuchus* from the matrix manually prior to rerunning the program, the analysis resulted in 2 MPTs, with a strict consensus tree of 98 steps (Figure 4). These results are more congruent with a recent study by Parker (2016a) using a larger character set, which also recovered *Coahomasuchus* in a polytomy with Typothoracinae. Surprisingly, *Gorgetosuchus* is recovered within Typothoracinae, a novel result as previous analyses have recovered it as a basal desmotosuchine (Heckert et al., 2015; Parker 2016a). Furthermore, with a width:length ratio of homologous dorsal paramedian osteoderms of  $\geq 3.5:1$ , the Pekin Formation *Coahomasuchus* is one of the stratigraphically oldest occurrences of a wide bodied aetosaur (Heckert et al., 2017).

**Discussion** – My analysis most closely matches work by Parker (2007, 2016a,b) and recovers all five of the recognized major clades of aetosaurs: Stagonolepididae, Aetosaurinae, Stagonolepidinae, Desmotosuchinae (Heckert & Lucas, 1999; Heckert & Lucas, 2000), and Typothoracinae (Parker, 2007). As in Parker (2016a), *Coahomasuchus* is recovered in a polytomy with *Aetosaurus*, as members of Aetosaurinae, and/or as a basal member of Typothoracinae when compared to Schoch and Desojo's (2016) analysis (Figures 3 & 4). If *Coahomasuchus* is a typothoracine, then it is the stratigraphically oldest one, and provides further evidence of an initial diversification of aetosaurs prior to the early Late Triassic (Nesbitt, 2003). Furthermore, the increased stability of *Coahomasuchus* with

the inclusion of updated and revised scorings echoes the importance of using the most recent and complete data (Parker, 2016a).

The more nested position of *Aetosaurus* within the aetosaur tree does not fit with early phylogenetic analyses of Aetosauria (Parrish, 1994; Heckert et al., 1996; Heckert and Lucas, 1999) but agrees with more recent work placing it within Stagonolepididae (Parker, 2007, 2016a). My analysis pulls *Stenomtyti* outside of Stagonolepididae, unlike other recent analyses (Schoch and Desojo, 2016; Parker, 2016a). The topology of Desmatosuchinae within my analysis resembles that of Schoch and Desojo (2016), but with a polytomy (Figures 3 & 4) and the liable position of *Lucasuchus*. These results do not greatly change accepted aetosaur relationships, but do differ from Parker's (2016a) placement of *Polesinesuchus* within Stagonolepidinae rather than Desmatosuchinae (Figure 3).

Stagonolepidinae, as recovered in my analysis, differs from the Heckert and Lucas (2000) definition of *Coahomasuchus kaleorum* and *Stagonolepis robertsoni*, but reflects the results of a more recent analysis (Schoch and Desojo, 2016). Contrary to Parker (2016a), I recover *Stagonolepis robertsoni* and *Stagonolepis wellsi* (*Calyptosuchus wellsi*) as sister taxa in a Stagonolepidinae clade, supporting the hypothesis of synonymizing the two (Heckert and Lucas, 2002) in a single genus, *Stagonolepis*. However, the placement of *Aetosauroides* as a basal aetosaur within my analysis supports the argument that it should not be considered a junior synonym of *Stagonolepis* (Desojo and Ezcurra, 2011; Parker, 2016a).

The placement of *Gorgetosuchus* within Typothoracinae, in a polytomy with *Redondasuchus* and *Typothorax*, is based on three osteoderm characters (characters 16, 17, 23—see below). This contrasts with other recent phylogenetic analysis which found *Gorgetosuchus* most similar to *Lucasuchus* and *Longosuchus*, though these similarities were also necessarily based entirely on osteoderm characters (Heckert et al., 2015; Parker, 2016a). All three of the synapomorphies (characters 16, 17 and 23 of Schoch and Desojo,

2016) which unite *Gorgetosuchus* with *Redondasuchus* and *Tyothorax* also appear in various places within Desmotosuchinae. Characters 16 and 17 are osteoderm ornamentation characters and scored for random patterning on paramedian osteoderms (16) and the ornamentation on the paramedian osteoderms consists of only small subcircular pits (Schoch and Desojo, 2016). Character 23 unites all three with presacral paramedian osteoderms that are strongly flexed ventrally (Schoch and Desojo, 2016). It is unclear if this is a genuine signal of a relationship with Tyothoracinae, or simply an example of convergent evolution, indicating the limited use of these characters as phylogenetic signals. With additional non-osteoderm material of *Gorgetosuchus* this discrepancy should be resolved, and the placement of *Gorgetosuchus* will likely stabilize (Heckert et al., 2015).

#### COMPUTED TOMOGRAPHIC RECONSTRUCTIONS

**Methods** – The original CT scans of the holotype specimen NCSM 23618 were completed at Siemens Medical Training Facility in Cary, North Carolina. The resulting DICOM data was processed and segmented using Avizo version 9.0.0 in the Paleontology and Geology Lab at the Nature Research Center in Raleigh, North Carolina. However, this original scan utilized a CT scanner with low detail (too few x-rays per mm). This, combined with the high density of the surrounding matrix, made the resulting CT images too low a resolution for the reconstructions to be used for character scoring, and most elements could not be reconstructed. A later scan was completed with the use of a CT scanner at the North Carolina State University College of Veterinary Medicine Diagnostic Facility. Here again the nature of the matrix interfered with the quality of the scans, creating beam hardening issues within the center of the specimen, although several new elements were revealed.

**Results** – Two separate CT reconstructions reveal multiple elements not seen on the exterior of the specimen, and provide more information on several elements that are partially

exposed on the surface, but continue into the matrix and disappear from view. For clarity, I discuss the two different scans separately.

From the original Siemens scan I was able to reconstruct a series of articulated vertebrae continuing anterior-medially beneath the vertebrae exposed on the surface, as well as an isolated vertebra (Figure 5). A limb element, possibly partially exposed, is seen on the right anterior portion of the specimen (Figure 5). The left humerus exposed on the surface was followed and shown to continue down into the matrix (Figure 5). Additionally, several ribs and other long bone fragments were identified and segmented throughout the specimen (Figure 5). The higher powered scans from NCSU Veterinary College capture many of the same elements including the “limb element”, which appears to be the right humerus, detailed from the original scans with two notable exceptions. The first is a series of seemingly articulated ribs along the left margin of the specimen (Figure 6). The second is a previously unseen element located within the matrix border surrounding the specimen on the left margin, lateral to the ribs, and appears to be the left ulna (Figure 6). Due to time constraints and the nature of the beam hardening, fewer total elements were reconstructed with this scan.

The left humerus is approximately 58 mm long and the preserved length of the right humerus visible on the scans is ~40 mm. There is approximately 40 mm of the left ulna preserved, though there is a fracture ~two-thirds of the way down the length of the ulna from the visible epiphysis, the other epiphysis is no longer present as the reconstruction terminates at the surface. The centra lengths in Figure 5 range between ~14 and 16 mm, encapsulating the value (~15 mm) reported by Heckert et al. (2017) for the dorsal centra. These lengths are comparable to the parasagittal lengths of nearby osteoderms (~13–20 mm), and fit with the common 1:1 ratio of vertebrae to osteoderms (Walker, 1961; Long and Murry, 1995; Desojo et al., 2013; Parker, 2016a; Heckert et al., 2017). There appear to be at least three articulated vertebrae not exposed on the surface, possibly four, and one isolated

vertebra (Figure 5). In the second scan, five articulated ribs are visible (Figure 6), one complete rib is visible from the original scan (Figure 5), and numerous small fragments can be found in both scans.

**Discussion** – This first look under the articulated osteoderms of an aetosaur produced as many challenges as successes. Though several elements could be reconstructed from beneath the osteoderms and within the surrounding matrix, the quality of the reconstructions does not allow for additional character scoring, or even significant qualitative description. The lack of resolution in the scans is due to a combination of compression of the specimen and density. The dorso-ventral compression of the specimen displaced or damaged several elements, evidenced by the multiple thin bone fragments found throughout the carapace (Figure 5). This also forced the osteoderms into close proximity with the internal skeleton, rendering differentiation of osteoderm and endoskeletal bone difficult. The dense matrix of iron-rich sandstone and conglomerate, as well as the thorough mineralization of the bone, results in a very small density difference between the fossil bones and the surrounding rock. Furthermore, the presence of iron-rich nodules caused beam hardening in both scans. Despite these complications, several new bones were digitally uncovered (ribs, vertebrae, left ulna, right humerus), and others were followed into the matrix (left humerus, dorsal vertebrae). This result indicates the potential to reveal important morphological data in other similarly preserved aetosaur specimens using CT reconstructions, especially in specimens with greater density differences between the bone and the encasing matrix. A possible candidate is a specimen of *Aetosaurus* from the Sanford Formation (NCSM 11756) described by Lucas et al. (1998). The specimen is an articulated, partial tail (Lucas et al., 1998), which may present a simpler subject.

## HISTOLOGY

**Background** – The first histologic study of aetosaurs, and one of few to include non-crocodylomorph pseudosuchian archosaurs, was conducted by de Ricqlès et al. (2003) in

an attempt to determine the origin(s) of endo- and ectothermy within Archosauria. Since then, at least six other studies have published on aetosaur histology, usually limited to one or two taxa and/or one or two specimens per taxon (Table 2). Previous studies have often focused on bone tissue variation and growth rates (e.g. Cerda and Desojo, 2011; Taborda et al., 2013). The histologic results have been used to infer reasons behind intraspecific variation of osteoderm ornamentation and explain different osteoderm morphologies (Parker et al., 2008; Taborda et al., 2015). However, many of these authors have also noted the difficulties of using LAGs to estimate age, and therefore growth rates and ontogenetic stage, because of remodeling in the internal core and basal cortex (e.g. Scheyer et al., 2014). LAGs are associated with annual interruptions growth in modern reptiles and can be correlated with similar preserved lines in fossil reptiles, such as aetosaurs (Cerda and Desojo, 2011; Taborda et al., 2013). Because modern crocodylians begin ossification of their osteoderms one year after hatching, one year is added to the number of LAGs obtained from aetosaur osteoderms for more accurate results (Taborda et al., 2013). With this study, *C. chathamensis* is now likely the second most sampled species of aetosaur, after *Aetosauroides scagliai* (Cerda and Desojo, 2010, 2011; Taborda et al., 2013, 2015).

Histological terms used herein are from Francillon-Vieillot et al. (1990) and tissue regions of aetosaur paramedian osteoderms come from Cerda and Desojo (2011). The three regions of a paramedian: external cortex, internal core, and basal cortex are more accurate convention for placement of tissues than dorsal/ventral (Cerda and Desojo, 2011). I refer to two general bone tissue types: woven fibred bone and parallel fibred bone. Woven fibred bone contains typically randomly distributes osteocytes which are usually rounded and oblong (Francillon-Vieillot et al., 1990). This bone type implies rapid osteogenesis (bone growth), resulting in the low level of organization (Francillon-Vieillot et al., 1990). Parallel fibred bone contains osteocytes in a variety of distributions, generally oriented in the same direction and run parallel to one another (Francillon-Vieillot et al., 1990). This bone type is

an intermediate between woven fibred and lamellar fibred bone, indicate a lower rate of growth than woven fibred bone and changes between the types are functionally linked to growth rate variations (Francillon-Vieillot et al., 1990). Primary osteons are vascular canals associated with original deposition of bone, indicating no reabsorption of bone (Francillon-Vieillot et al., 1990). A secondary osteon is an erosional opening in vascular canals as part of Haversian systems which are large openings of holes found in rapidly growing young bone (Francillon-Vieillot et al. 1990).

**Methods** – I undertook histological examination, sampling a paramedian osteoderm physically isolated from the holotype (NCSM 23618) during preparation, as well as five osteoderms (two paramedian, one lateral, and two of uncertain position) and two incomplete limb bones (tibia and fibula) from referred specimens discovered at the holotype locality (Table 3). These analyses were performed following standard petrographic thin-sectioning of fossil material (e.g. Wilson, 1994; Lamm, 2013). The associated osteoderm specimens had all been damaged by a rock saw during their excavation, making them ideal to sample transversely, longitudinally, or both, bisecting the center of ossification and/or the anterior bar or posterior margin, depending on preservation, along previous cuts as done in other studies of aetosaur osteoderm histology (e.g., Taborda et al., 2013). The partial limbs are both broken across the shaft, and are ideal for transverse sections taken near mid-shaft (e.g., de Ricqlès et al., 2003; Padian et al., 2013). Prior to sectioning, all specimens were photographed and measured according to protocols developed by Martz (2002), and NCSM 23618 was molded in Smooth-On: Mold Max 20. Then, the specimens were embedded in polyurethane resin to provide structural support. Specimens were sectioned with a circular saw, attached to glass slides with the same resin used for embedding, and polished to thickness of 60-80  $\mu\text{m}$ , following Scheyer et al.'s (2014) technique for examining Triassic armor and other guidelines described by Lamm (2013).

**Results** – Ten histologic slides were made in total, two of an osteoderm from the holotype of *C. chathamensis* and eight of referred material (Table 3).

*Ontogeny* – LAG counts for the associated material ranged from three to seven, and one or possibly two LAGs in the type specimen. Therefore, our material represents a range of ages from at least two to eight years old among several individuals. LAGs were most apparent on the appendicular material (Figure 7) with four LAGs visible on NCSM 16441 (partial fibula, Figure 7B) and as many as seven LAGs visible on NCSM 19765 (partial tibia, Figure 7C). Transverse sections (Figure 8) of referred osteoderms yielded a range of LAG counts from three (NCSM 18819A, Figure 8B) to a minimum of five (NCSM 20827, Figure 8C).

Parasagittal sections of referred osteoderms (Figure 9) exhibited LAG counts of three (NCSM 16435 and 18819B, not illustrated), four (NCSM 21175, Figure 9B), to as many as six (NCSM 26204, Figure 9D). The youngest individual sampled appears to be the type specimen (NCSM 23618) which reveals a possible one to two LAGs (Figure 10).

In the limb bones (fibula and tibia), the majority of the LAGs appear near the outer layers of tissue (expanded upon below) and in the osteoderms the LAGS are usually visible throughout, but most definite in the basal cortex (expanded upon below).

*Tissue Descriptions* – The fibula and tibia are both approximately elliptical, with their marrow cavities filled in with minerals, predominately calcite (Figure 7). As seen in aetosaurs described by de Ricqlès et al. (2003), vascularization increases towards the internal cortex, forming woven fibred bone. The inner units of bone show little evidence of Haversian reconstruction (secondary osteons) suggesting little to no tissue replacement occurred in the preserved tissues of these two limb bones. The outer layers of bone that comprise the majority of the LAGs in these two specimens appears to be lamellar-zonal (parallel fibred bone) with occasional longitudinal to reticular primary osteons (Figure 7A). The presence of multiple tissue types suggests a change in growth through ontogeny (de Ricqlès et al., 2003).

The osteoderms also exhibit bone microstructural features previously described in other histologic studies (e.g. de Ricqlès, 2003; Cerda and Desojo, 2011; Scheyer et al., 2014). As in Cerda and Desojo (2011), some of the sectioned osteoderms could be divided into three discrete regions based on bone microstructure, such as NCSM 21175 (Figure 9A, B). The basal cortex of NCSM 21175 exhibits the best preserved LAGs and is composed of parallel fibred bone tissue with relatively poor vascularization compared to the rest of the osteoderm. The internal core of NCSM 21175 is made of highly vascularized woven fibred bone with primary osteons oriented subparallel to the main axis of the osteoderm. The external cortex of NCSM 21175 is made of highly compact, parallel fibred bone with very little vascularization.

Other osteoderms (e.g. NCSM 20827 and 26204) exhibit a definite basal cortex of poorly vascularized parallel fibred bone and an internal core of highly vascularized woven fibred bone, but appear to lack the external cortex (Figures 8B, C, 9C, D). The lateral osteoderm in the study, NCSM 18819, has a highly vascularized, woven fibred core of bone surrounded by continuous, poorly vascularized, parallel fibred bone (Figure 8A, B), but lacks a distinct external cortex and basal cortex, as depicted by Cerda and Desojo (2011). Rather the basal and external cortex seem to form a continuum around the internal cortex, instead of two separate bands. Additionally, the lateral margin of the internal core appears to be more greatly vascularized than the rest of the internal core (Figure 8B). This corresponds to the spine present on the left lateral external surface and may represent the center of ossification in lateral osteoderms, similar to process of osteoderm growth described by Martz (2002) in which growth originates at one location, and continues laterally and medially from this location (center of ossification) usually associated with the external eminence of Cerda and Desojo (2011).

**Discussion** – Given paramedian osteoderm widths of up to 90 mm in the type specimen of *C. chathamensis* (Heckert et al., 2017), and 70 mm wide for the sectioned osteoderm in the

study, it is clear that *C. chathamensis* was growing rapidly compared to similarly sized aetosaurs. For example, the type specimen of *Aetosauroides scagliai* (up to 92 mm paramedian osteoderm widths) contained five unambiguous LAGs (Taborda et al., 2015). Thus, at 6+ years of age, this specimen was no larger (in terms of maximum paramedian osteoderm width) than the younger (~3 years?) holotype of *C. chathamensis*. Such rapid growth may explain, in part, the diagnostic faint radial ornamentation of subparallel grooves and ridges on the paramedian osteoderms of *C. chathamensis* (Heckert, 2015).

The presence of rapid growth rates has been proposed to be the primitive condition of archosauriforms, with later reduction in some Pseudosuchian groups, and further reduction in crocodylians (de Ricqlès et al., 2003, 2008). However, aetosaurs were still found to have a growth rate similar to that of modern crocodylians (de Ricqlès et al., 2003). This finding has been repeated in other work (e.g. Parker et al., 2008) though other authors have found slower growth rates of aetosaurs when compared to modern crocodylians (e.g. Taborda et al., 2013). The histology reported here adds additional variation to the known patterns of aetosaur growth, with *C. chathamensis* appearing to attain the same size as *Aetosauroides scagliai* (Taborda et al., 2015) in 1/3 to 1/2 the time. If rapid growth did arise in Archosauriformes prior to the origin of Archosauria, then it is plausible for multiple growth strategies to arise within a single diverse clade, as suggested by other authors (e.g. Scheyer et al., 2014). Further research needs to be completed within an evolutionary framework of aetosaurs to investigate any possible trends to the apparent variation in growth strategies.

An additional issue this study raises is *C. chathamensis* is a juvenile, and if *C. kahleorum* is as well, and they both are known from deposits with other aetosaurs (e.g. *Lucasuchus*, *Longosuchus*, *Gorgetosuchus*), then is *Coahomasuchus* a juvenile of one of these taxa? Traits attributed to *Coahomasuchus* as being plesiomorphic (e.g. Parker 2007, Parker, 2016a) have instead been suggested to be juvenile characters (e.g. Schoch and Desojo, 2016). A systematic sampling of aetosaur osteoderms of multiple taxa from the

same locality could help resolve this dispute (if, for example, juvenile *Lucasuchus*, *Longosuchus*, *Gorgetosuchus* are found with osteoderms not resembling *Coahomasuchus*).

## LITERATURE CITED

- Brochu, C. A. 1996. Closure of neurocentral sutures during crocodylian ontogeny: implications for maturity assessment in fossil archosaurs. *Journal of Vertebrate Paleontology* 16(1), 49-62.
- Campbell, M. R., and Kimball, K. K. 1923. The Deep River coal field of North Carolina. *North Carolina Geological and Economic Survey Bulletin* 33, 1-95.
- Cerda, I.A. and Desojo, J.B. 2010. Dermal armour histology of *Aetosauroides* Casamiquela, 1960 (Archosauria: Aetosauria) from the Upper Triassic of Argentina and Brazil. *Ameghiniana* 47, 70R.
- Cerda, I. A., and Desojo, J. B. 2011. Dermal armour histology of aetosaurs (Archosauria: Pseudosuchia), from the Upper Triassic of Argentina and Brazil. *Lethaia* 44(4), 417-428.
- Cornet, B. 1993. Applications and limitations of palynology in age, climatic, and paleoenvironmental analyses of Triassic sequences in North America. *New Mexico Museum of Natural History and Science Bulletin* 3, 75-93.
- Desojo, J.B. and Ezcurra, M.D. 2011. A reappraisal of the taxonomic status of *Aetosauroides* (Archosauria: Aetosauria) specimens from the Late Triassic of South America and their proposed synonymy with *Stagonolepis*. *Journal of Vertebrate Paleontology* 31, 596-609.
- Desojo, J. B., Heckert, A. B., Martz, J. W., Parker, W. G., Schoch, R. R., Small, B. J., and Sulej, T. 2013. Aetosauria: a clade of armoured pseudosuchians from the Upper Triassic continental beds. *Geological Society, London, Special Publications* 379(1), 203-239.
- de Ricqlès, A. J., Padian, K., and Horner, J. R. 2003. On the bone histology of some Triassic pseudosuchian archosaurs and related taxa. In *Annales de Paléontologie* 89(2), 67-101.

- de Ricqlès, A., Padian, K., Knoll, F., and Horner, J. R. 2008. On the origin of high growth rates in archosaurs and their ancient relatives: Complementary histological studies on Triassic archosauriforms and the problem of a “phylogenetic signal” in bone histology. In *Annales de Paléontologie* 94(2), 57-76.
- Drymala, S. M., and Zanno, L. E. 2016. Osteology of *Carnufex carolinensis* (Archosauria: Psuedosuchia) from the Pekin Formation of North Carolina and its implications for early crocodylomorph evolution. *PLoS ONE* 11(6), e0157528.
- Francillon-Vieillot, H., de Buffrénil, V., Castanet, J., Ge´raudie, J., Meunier, F.J., Sire, J.Y., Zylberberg, L. and de Ricqlès, A. 1990. Microstructure and mineralization of vertebrate skeletal tissues. In Carter, J.G. (ed.): *Skeletal Biomineralization: Patterns, Processes and Evolutionary Trends*, 471–548. Van Nostrand Reinhold, New York.
- Furin, S., Preto, N., Rigo, M., Roghi, G., Gianolla, P., Crowley, J. L., and Bowring, S. A. 2006. High-precision U-Pb zircon age from the Triassic of Italy: Implications for the Triassic time scale and the Carnian origin of calcareous nannoplankton and dinosaurs. *Geology* 34, 1009-1012.
- Goloboff, P.A., Farris, J.S., and Nixon, K.C. 2008. TNT, a free program for phylogenetic analysis. *Cladistics* 24, 774-786.
- Green, J. L., Schneider, V. P., Scheitzer, M., and Clarke, J. 2005. New evidence for non-*Placerias* dicynodonts in the Late Triassic (Carnian-Norian) of North America. *Journal of Vertebrate Paleontology* v. 25(3), 65-66.
- Green, J. L. 2012. Bone and dental histology of Late Triassic dicynodonts from North America, in Chinsamy-Turan, A., ed., *Forerunners of mammals: Radiation, Histology, Biology*. *Bloomington, Indiana University Press* 178–196.
- Heckert, A. B., Hunt, A. P., and Lucas, S. G. 1996. Redescription of *Redondasuchus reseri*, a Late Triassic aetosaur (Reptilia: Archosauria) from New Mexico (USA), and the biochronology and phylogeny of aetosaurs. *Geobios* 29(5), 619-632.

- Heckert, A. B., and Lucas, S. G. 1999. A new aetosaur (Reptilia: Archosauria) from the Upper Triassic of Texas and the phylogeny of aetosaurs. *Journal of Vertebrate Paleontology* 19(1), 50-68.
- Heckert, A. B., and Lucas, S. G. 2000. Taxonomy, phylogeny, biostratigraphy, biochronology, paleobiogeography, and evolution of the Late Triassic Aetosauria (Archosauria: Crurotarsi). *Zentralblatt für Geologie und Paläontologie, Teil I* 1998(11-12), 1539-1587.
- Heckert, A. B., and Lucas, S. G. 2002. South American occurrences of the Adamanian (Late Triassic: latest Carnian) index taxon *Stagonolepis* (Archosauria: Aetosauria) and their biochronological significance. *Journal of Paleontology* 76(5), 852-863.
- Heckert, A. B. 2015. Variation in the ornamentation pattern of aetosaur (Archosauria:Suchia) osteoderms: taxonomic and paleobiological implications. *Journal of Vertebrate Paleontology, SVP Program and Abstracts Book 2015*, 141.
- Heckert, A.B., Schneider, V.P., Fraser, N.C., and Webb, R.A. 2015. A new aetosaur (Archosauria: Suchia) from the Upper Triassic Pekin Formation, Deep River Basin, North Carolina, U.S.A., and its implications for early aetosaur evolution. *Journal of Vertebrate Paleontology* 35(1):e881831 DOI 10.1080/02724634.2014.881831.
- Heckert, A. B., Fraser, N. C., and Schneider, V. P. 2017. A new species of *Coahomasuchus* (Archosauria:Aetosauria) from the Upper Triassic Pekin Formation, Deep River Basin, North Carolina. *Journal of Paleontology* 91(1), 162-178.
- Huber, P., Lucas, S. G., and Hunt, A. P.1993. Revised age and correlation of the Upper Triassic Chatham Group (Deep River Basin, Newark Supergroup), North Carolina. *Southeastern Geology* 33, 171-193.
- Irmis, R. B., 2007, Axial skeleton ontogeny in the Parasuchia (Archosauria:Pseudosuchia) and its implications for ontogenetic determination in archosaurs. *Journal of Vertebrate Paleontology* 27(2), 350-361.

- Kawashima, T., Thorington, R. W., Bohaska, P. W., Chen, Y. J., and Sato, F. 2015. Anatomy of shoulder girdle muscle modifications and walking adaptation in the Scaly Chinese Pangolin (*Manis pentadactyla pentadactyla*: Pholidota) compared with the partially osteoderm-clad armadillos (Dasypodidae). *The Anatomical Record* 298(7), 1217-1236.
- Lamm, E. T. 2013. Preparation and sectioning, in Padian, K., and Lamm, E.-T., eds., Bone histology of fossil tetrapods: advancing methods, analysis, and interpretation. *Berkeley, University of California Press* 35-54.
- Litwin, R. J., and Ash, S. R. 1993. Revision of the biostratigraphy of the Chatham Group (Upper Triassic), Deep River basin, North Carolina, USA. *Review of Palaeobotany and Palynology* 77, 75-95.
- Liu, J., and Sues, H. D. 2010. Dentition and tooth replacement of *Boreogomphodon* (Cynodontia: Traversodontidae) from the Upper Triassic of North Carolina, USA. *Vertebrata Palasiatica* 48, 169-184.
- Long, R. A., and Murry, P. A. 1995. Late Triassic (Carnian and Norian) tetrapods from the southwestern United States. *New Mexico Museum of Natural History and Science Bulletin* 4, 254.
- Lucas, S. G., Heckert, A. B., and Huber, P. 1998. *Aetosaurus* (Archosauromorpha) from the Upper Triassic of the Newark Supergroup, eastern United States, and its biochronological significance. *Palaeontology* 41(6), 1215-1230.
- Lucas, S. G., and Huber, P. 2003. Vertebrate biostratigraphy and biochronology of the nonmarine Late Triassic, in Le Tourneau, P.M., and Olsen, P. E., eds., The great rift valleys of Pangea in Eastern North America: Sedimentology, Stratigraphy, and Paleontology. *New York, Columbia University Press* 143-191.
- Lucas, S. G. 2010. ed., The Triassic timescale. *Geological Society, London, Special Publications: London, The Geological Society of London.* 334, 514.

- Lucas, S. G., Tanner, L. H., Kozur, H. W., Weems, R. E., and Heckert, A. B. 2012. The Late Triassic timescale: Age and correlation of the Carnian-Norian boundary. *Earth-Science Reviews* 114, 1-18.
- Martz, J. W. 2002. The morphology and ontogeny of *Typosuchus coccinarum* (Archosauria, Stagonolepididae) from the Upper Triassic of the American Southwest (Doctoral dissertation, Texas Tech University).
- Muttoni, G., Kent, D. V., Olsen, P. E., Stefano, P. d., Lowrie, W., Bernasconi, S. M., and Hernández, F. M. 2004. Tethyan magnetostratigraphy from Pizzo Mondello (Sicily) and correlation to the Late Triassic Newark astrochronological polarity time scale. *Geological Society of America Bulletin* 116, 1043-1058.
- Nesbitt, S. J. 2003. *Arizonasaurus* and its implications for archosaur divergence. *Proceedings of the Royal Society of London B: Biological Sciences* 270(Suppl 2), 234-237.
- Olsen, P. E., Froehlich, A. J., Daniels, D. L., Smoot, J. P., and Gore, P. J. W. 1991. Rift basins of early Mesozoic age, in Horton, J. W., Jr., and Zullo, V. A., eds., *Geology of the Carolinas*. Knoxville, University of Tennessee Press, 142-170.
- Olsen, P. E. 1997. Stratigraphic record of the early Mesozoic break up of Pangea in the Laurasia-Gondwana rift system. *Annual Review of Earth and Planetary Sciences* 25, 337-401.
- Padian, K., Lamm, E. T., and Werning, S. 2013. Selection of specimens, in Padian, K., and Lamm, E.-T., eds., *Bone histology of fossil tetrapods: advancing methods, analysis, and interpretation*. Berkeley, University of California Press 35-54.
- Parker, W.G. 2007. Reassessment of the aetosaur "*Desmatosuchus*" *chamaensis* with a reanalysis of the phylogeny of the Aetosauria (Archosauria: Pseudosuchia). *Journal of Systematic Palaeontology* 5(1), 5-28. DOI 10.1017/S1477201906001994.

- Parker, W. G., Stocker, M. R., and Irmis, R. B. 2008. A new desmotosuchine aetosaur (Archosauria: Suchia) from the Upper Triassic Tecovas Formation (Dockum Group) of Texas. *Journal of Vertebrate Paleontology* 28(3), 692-701.
- Parker, W. G. 2016a. Revised phylogenetic analysis of the Aetosauria (Archosauria: Pseudosuchia); assessing the effects of incongruent morphological character sets. *PeerJ* 4, e1583.
- Parker, W. G. 2016b. Osteology of the Late Triassic aetosaur *Scutarx deltatylus* (Archosauria: Pseudosuchia). *PeerJ* 4, e2411.
- Parrish, J. M. 1994. Cranial osteology of *Longosuchus meadei* and the phylogeny and distribution of the Aetosauria. *Journal of Vertebrate Paleontology* 14(2), 196-209.
- Rogers, K. C., D'Emic, M., Rogers, R., Vickaryous, M., and Cagan, A. 2011. Sauropod dinosaur osteoderms from the Late Cretaceous of Madagascar. *Nature communications* 2, 564.
- Scheyer, T. M., Desojo, J.B. and Cerda, I. A. 2011. Comparative palaeohistology of Triassic rauisuchian and aetosaurian osteoderms (Archosauria: Pseudosuchia). 71<sup>st</sup> Annual Meeting of the Society of Vertebrate Paleontology, Las Vegas, USA. *Journal of Vertebrate Paleontology* 31, 49A.
- Scheyer, T. M., Desojo, J. B., & Cerda, I. A. 2014. Bone histology of phytosaur, aetosaur, and other archosauriform osteoderms (Eureptilia, Archosauromorpha). *The Anatomical Record* 297(2), 240-260.
- Schoch, R. R., and Desojo, J. B. 2016. Cranial anatomy of the aetosaur *Paratypothorax andressorum* Long & Ballew, 1985, from the Upper Triassic of Germany and its bearing on aetosaur phylogeny. *Neues Jahrbuch für Geologie und Paläontologie-Abhandlungen* 279(1), 73-95.

- Taborda, J. R., Cerda, I. A., and Desojo, J. B. 2013. Growth curve of *Aetosauroides scagliai* Casamiquela 1960 (Pseudosuchia: Aetosauria) inferred from osteoderm histology. *Geological Society, London, Special Publications* 379(1), 413-423.
- Taborda, J. R., Heckert, A. B., and Desojo, J. B. 2015. Intraspecific variation in *Aetosauroides scagliai* Casamiquela (Archosauria: Aetosauria) from the Upper Triassic of Argentina and Brazil: An example of sexual dimorphism? *Ameghiniana* 52(2), 173-187.
- Walker, A. D. 1961. Triassic reptiles from the Elgin area: *Stagonolepis*, *Dasygnathus*, and their allies. *Philosophical Transactions of the Royal Society of London, B* 244, 103-204.
- Weems, R. E., and Olsen, P. E. 1997. Synthesis and revision of groups within the Newark Supergroup, eastern North America. *Geological Society of America Bulletin* 109, 195-209.
- Wilson, J. W. 1994. Histological techniques. *Vertebrate paleontological techniques* 1, 205-234.
- Whiteside, J. H., Grogan, D. S., Olsen, P. E., and Kent, D. V. 2011. Climatically driven biogeographic provinces of Late Triassic tropical Pangea. *Proceedings of the National Academy of Sciences* 108(22), 8972-8977.
- Zanno, L. E., Drymala, S., Nesbitt, S. J., and Schneider, V. P. 2015. Early crocodylomorph increases top tier predator diversity during rise of dinosaurs. *Science Reports* 5(9276), <http://dx.doi.org/10.1038/srep09276>.

## TABLES

NCSM Number	Element
16368	Six osteoderms (only largest paramedian definitive)
16434	Partial left paramedian osteoderm
16436	Block with six osteoderms (one left paramedian)
16445-3	left paramedian osteoderm
16472	Dorsal paramedian osteoderm
18709	Partial right paramedian osteoderm
19302	Right paramedian osteoderm
19303	Posterior dorsal paramedian
19633	Partial lateral osteoderm
19635	Right paramedian osteoderm
20406	Partial right paramedian osteoderm
20797	Partial right paramedian osteoderm
20799	Ventral osteoderm
20827	Partial right paramedian osteoderm
20908	Right paramedian osteoderm
21062	Partial paramedian osteoderm
21071	Partial left lateral osteoderm
21137	Left paramedian osteoderm
21180	Partial left paramedian osteoderm
21274	Left caudal lateral osteoderm and impression
21569	Right(?) lateral osteoderm
21602	Partial right paramedian osteoderm
21604	Left paramedian osteoderm
24808	Partial ventral(?) osteoderm
26014	Ventral osteoderm
26023	Partial osteoderm
26203	Partial lateral osteoderm

**Table 1:** Complete list of all definitely *C. chathamensis* specimens in the NCSM collections not previously discussed in Heckert et al. (2017), or referred to later in this study (see Table 3) with a corresponding element label. At least the same amount of material is possibly *C. chathamensis* within the NCSM collections.

Study	Taxa	Skeletal Element(s)
de Ricqlès et al. (2003)	<i>Desmatosuchus</i> sp. <i>Stagonolepis</i> sp. <i>Typothorax</i> sp.	Humerus and radius Femur Radius
Parker et al. (2008)	<i>Sierritasuchus macalpini</i>	Paramedian osteoderm
Cerda and Desojo (2010)	<i>Aetosauroides scagliai</i>	Paramedian osteoderms (2)
Cerda and Desojo (2011)	<i>Aetosauroides scagliai</i> Aetosaurinae indet.	Paramedian osteoderms (2) Paramedian (9) and lateral osteoderm(s)
Taborda et al. (2013)	<i>Aetosauroides scagliai</i> <i>Aetobarbakinoides brasiliensis</i> Aetosaurinae indet. <i>Aetosaurus ferratus</i> <i>Paratypothorax</i> sp.	Paramedian, ventral, lateral, and appendicular osteoderms from Scheyer et al. (2011)
Scheyer et al. (2014)	<i>Adamanasuchus eisenhardtae</i> <i>Aetosaurus ferratus</i> <i>Calyptosuchus wellsi</i> <i>Desmatosuchus smalli</i> <i>Desmatosuchus spurensis</i> <i>Paratypothorax andressorum</i> <i>Paratypothorax</i> sp. <i>Stagonolepis olenkae</i> Stagonolepididae unnamed <i>Tecovasuchus chatterjeei</i> <i>Typothorax</i> sp.	Paramedian osteoderm Paramedian osteoderm Paramedian osteoderm Paramedian osteoderm Cervical lateral osteoderm Paramedian osteoderm Paramedian osteoderms (3) Paramedian osteoderms (4) Osteoderm Paramedian osteoderm Paramedian osteoderms (3)
Taborda et al. (2015)	<i>Aetosauroides scagliai</i>	Comparison of data from Cerda and Desojo (2010; 2011) and Scheyer et al. (2014).

**Table 2:** Summary of past histological studies involving aetosaurs. Most focus on paramedian osteoderms and only a few taxa, with the notable exception of Scheyer et al. (2014). However, even Scheyer et al. (2014) only used one sample for most of the taxa, often from fragmentary osteoderms.

NCSM #	Element	Section types
23618	Paramedian osteoderm, isolated from holotype	Transverse and parasagittal
20827	Paramedian osteoderm	Transverse
26204	Paramedian osteoderm	Parasagittal
18819	Lateral osteoderm	Transverse and parasagittal
16435	Indeterminate osteoderm	Parasagittal
21175	Indeterminate osteoderm (paramedian?) associated with NCSM 21173	Parasagittal
19765	Tibia (incomplete)	Transverse, mid-shaft
16441	Fibula (incomplete)	Transverse, mid-shaft

**Table 3:** Complete set of specimens used in histologic study and how they were sectioned.

## FIGURES

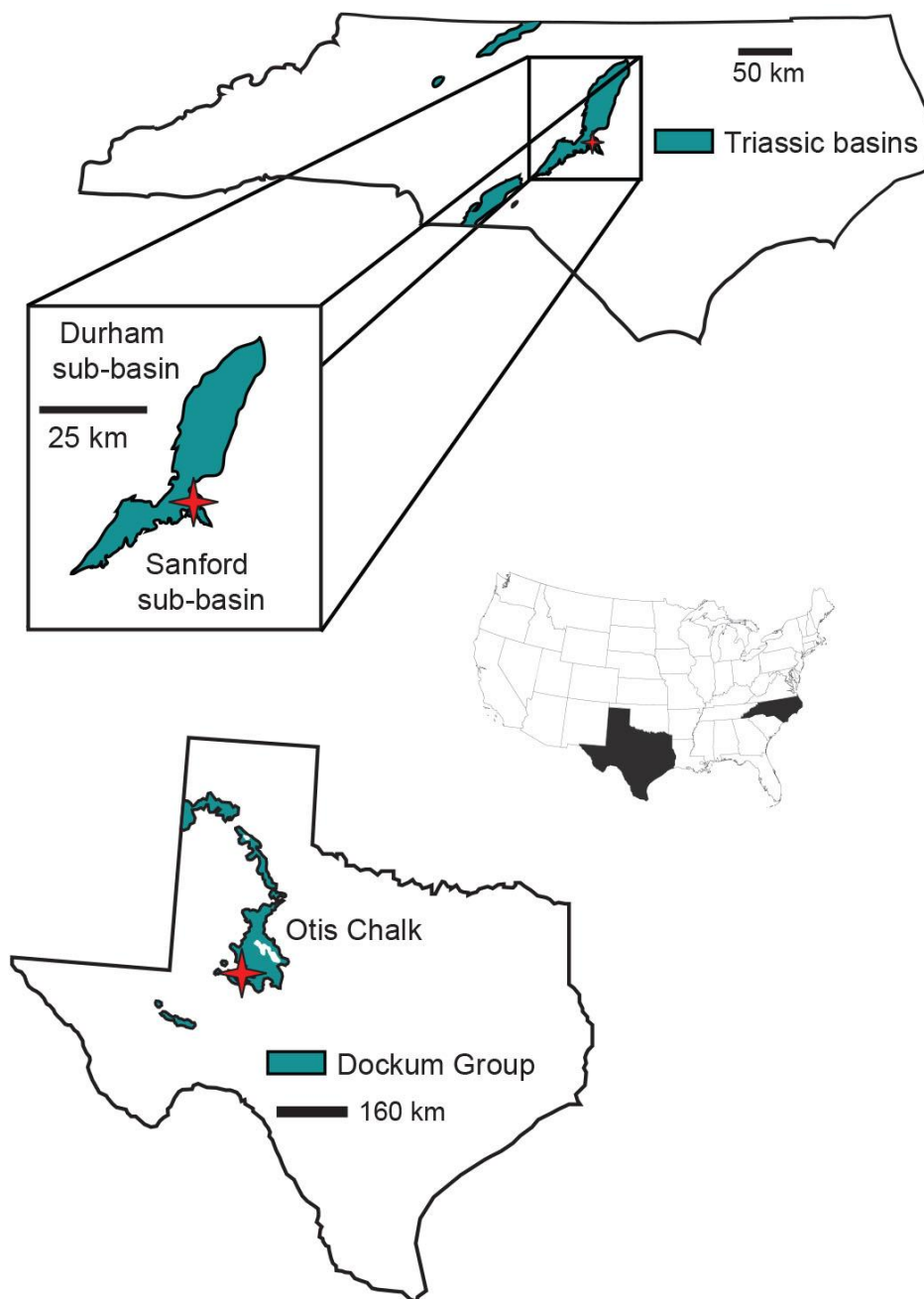


**Figure 1:** Generalized map of North Carolina’s Triassic Basins showing the location of the *Coahomasuchus chathamensis* specimen within the Deep River Basin, modified from Heckert et al. (2017, Fig. 1.1). Bottom - Generalized map of the Dockum Group of Texas with locality of original *Coahomasuchus kahleorum* specimen, based on Heckert and Lucas (1999, Fig. 2).

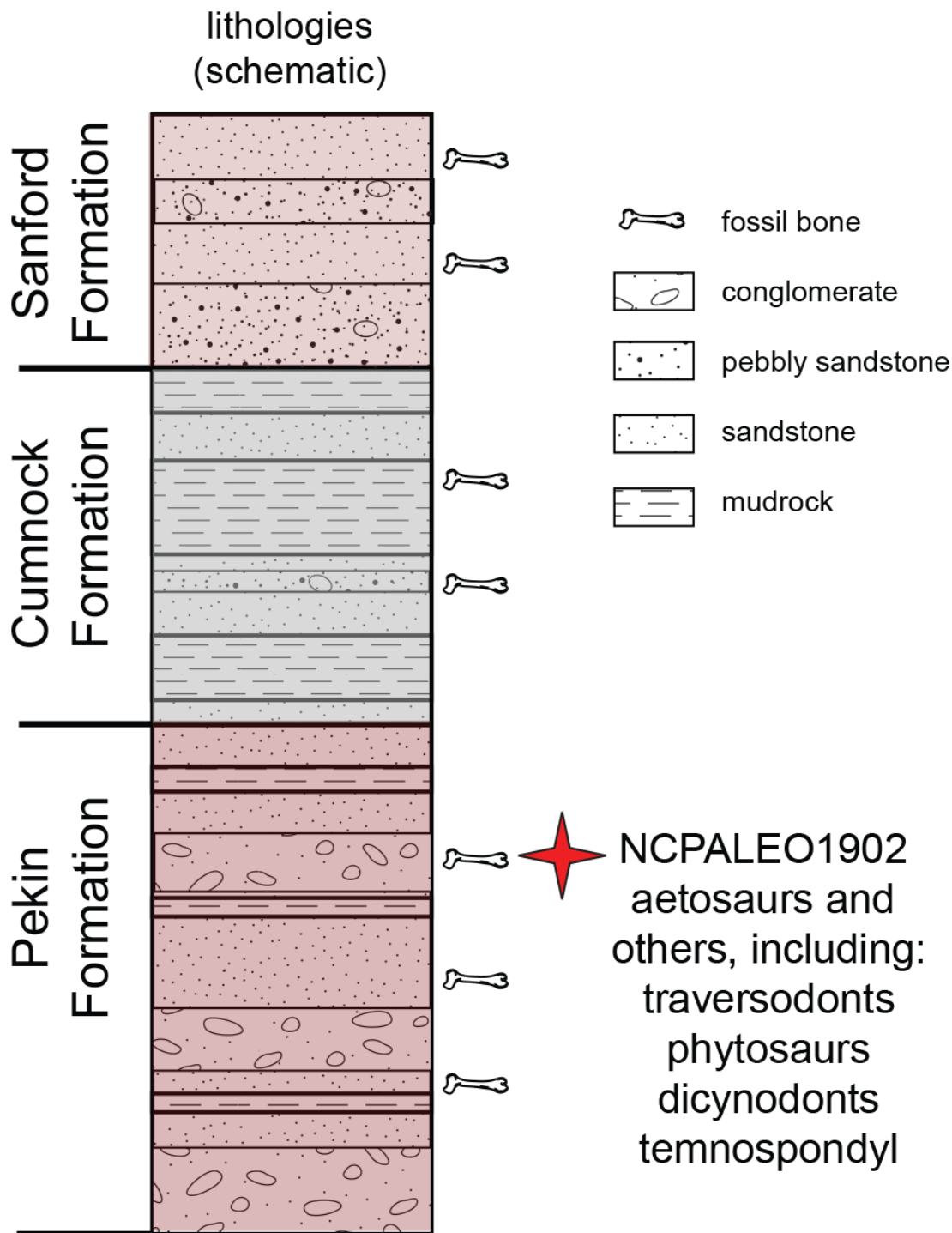


**Figure 2:** Simplified stratigraphic section of the Sanford sub-basin showing the location of *Coahomasuchus chathamensis*, from Heckert et al. (2017, Fig. 1.3).

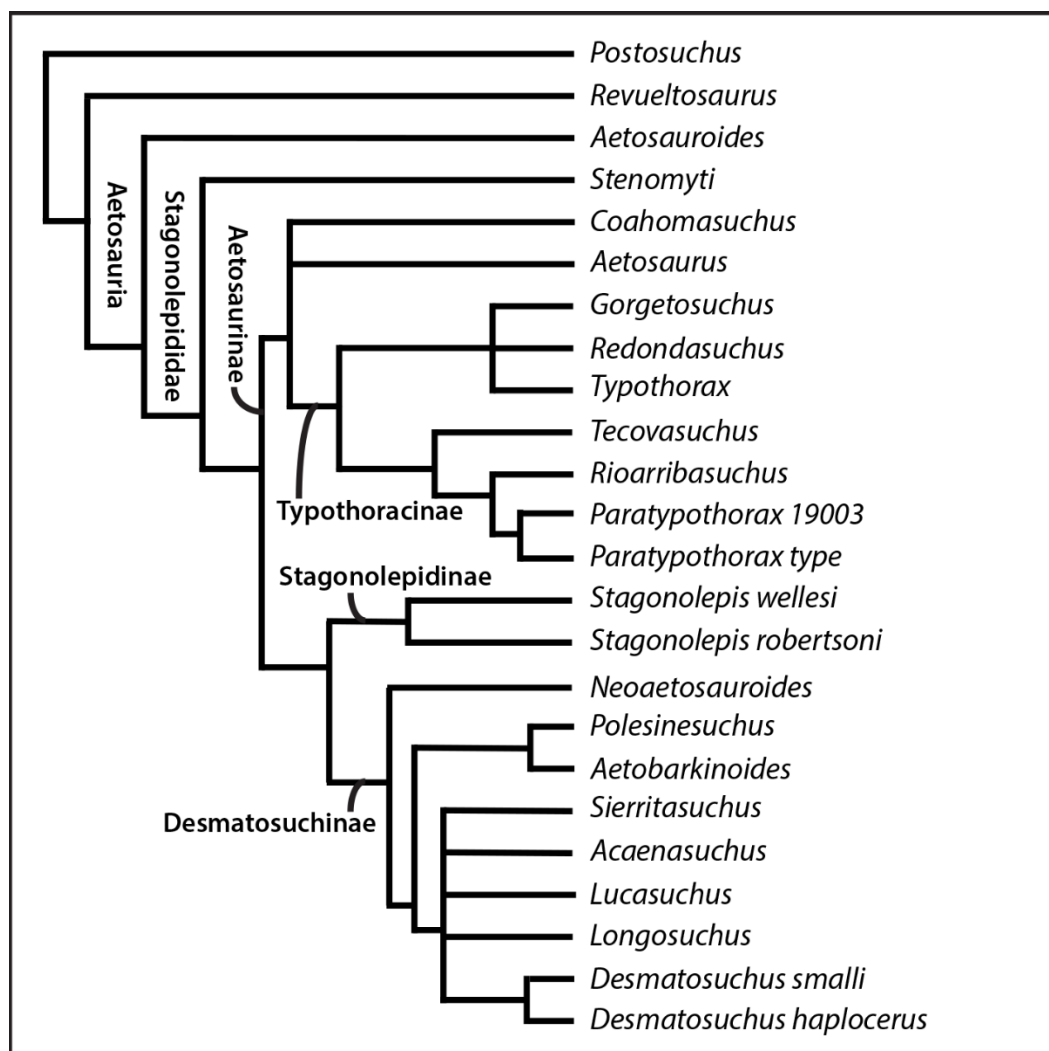


**Figure 3:** Strict consensus of updated matrix (100 steps) from Schoch and Desojo (2016) including *Lucasuchus*. *Aetobarkinoides* (and possibly *Polesinesuchus*) may be removed from Desmatosuchinae once more osteoderm characters can be scored. *Aetosaurus* is far removed from a monophyletic *Paratypothorax* in this analysis.

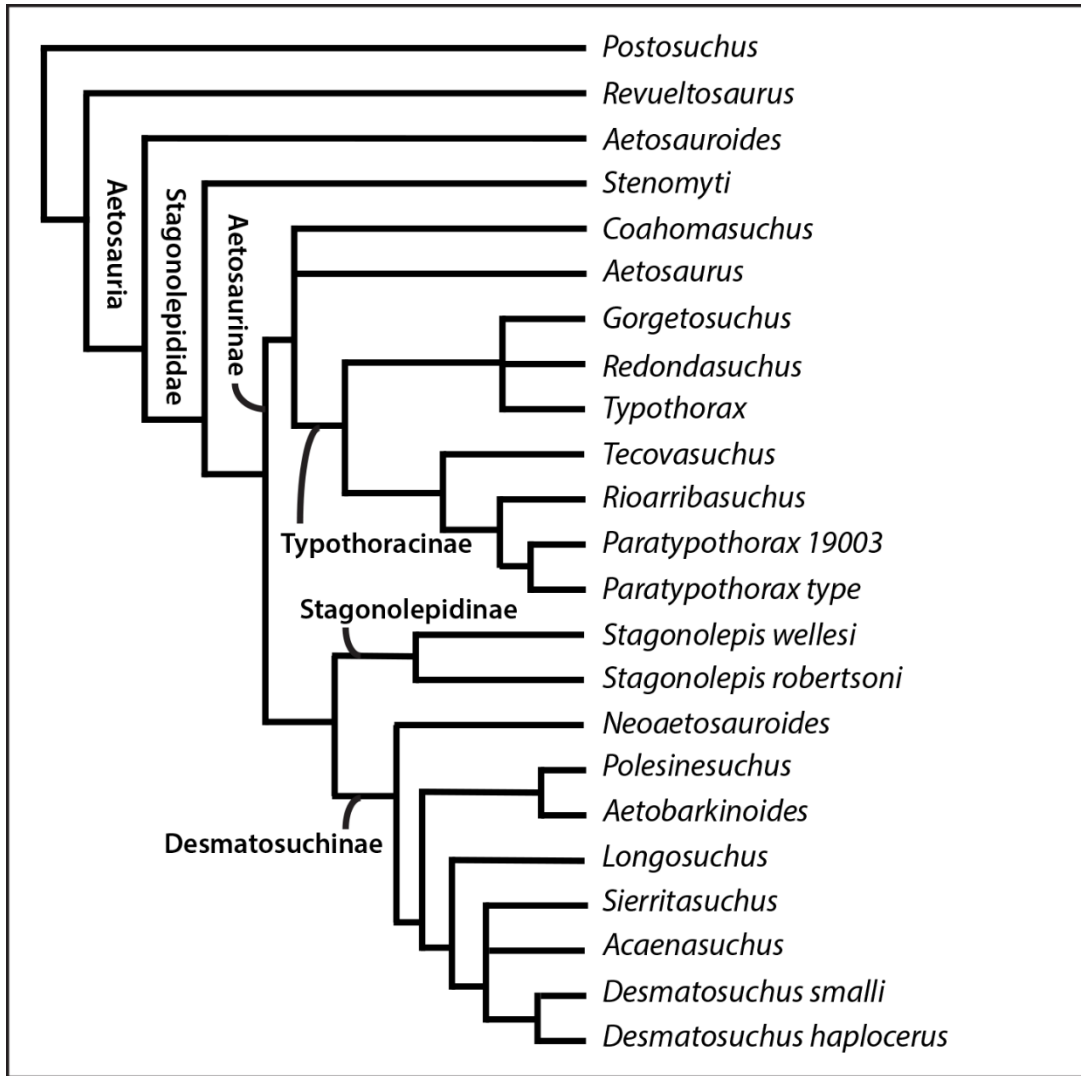


**Figure 4:** Strict consensus of updated matrix (98 steps) from Schoch and Desojo (2016) with *Lucasuchus* pruned from analysis.



**Figure 5:** Overview (ventral) of segmentation results from Siemens scan. hu = humerus; r = rib(s); vt = vertebra(e). Link to video of element rotating in 3D space below.

<https://drive.google.com/open?id=0B0UYKe3Paw3ERXB3QWNWWEwyZzQ>

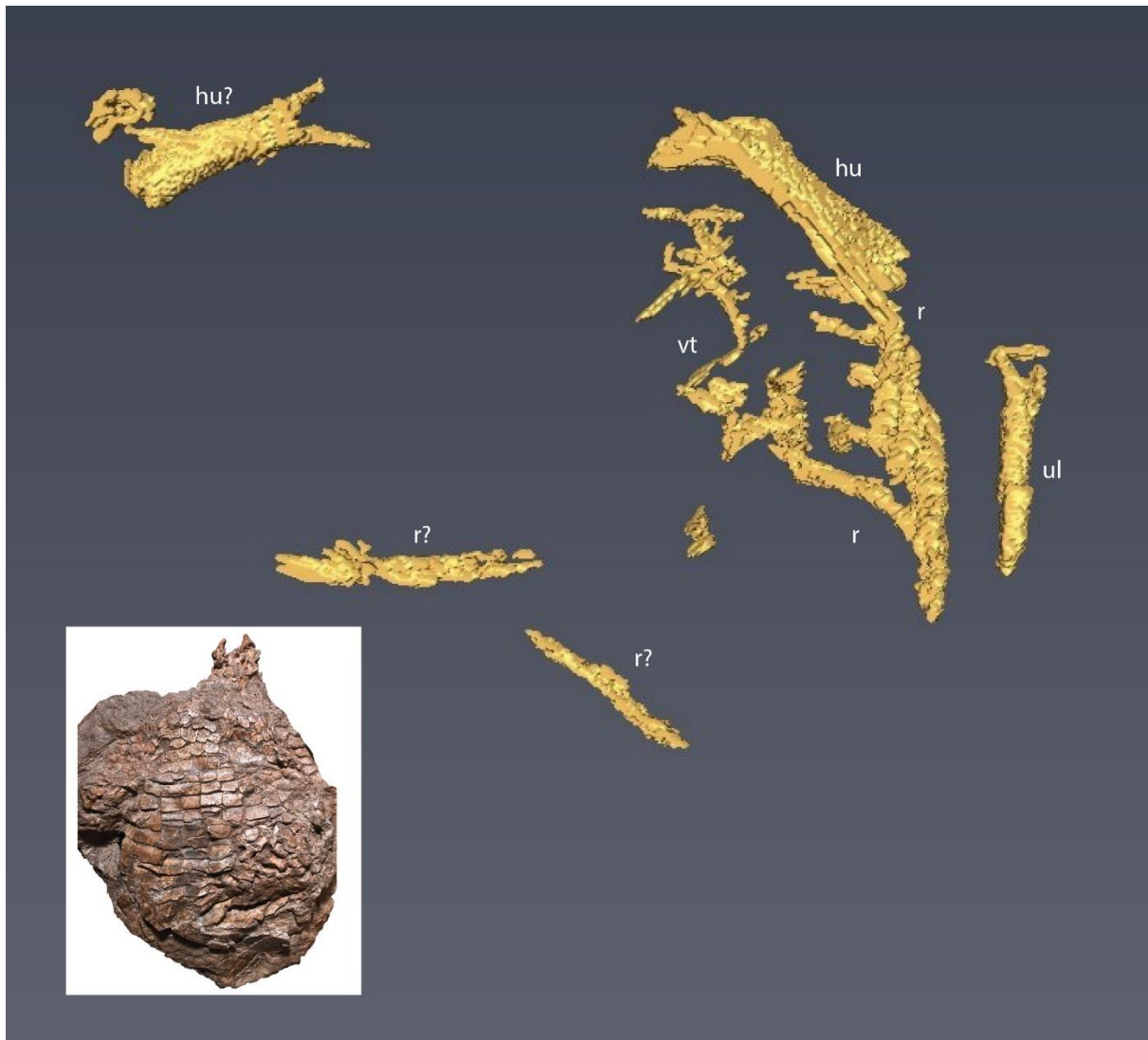


**Figure 6:** Overview (ventral) of segmentation results from NCSU Veterinary College scan.

hu = humerus; r = rib(s); vt = vertebra(e); ul = ulna.

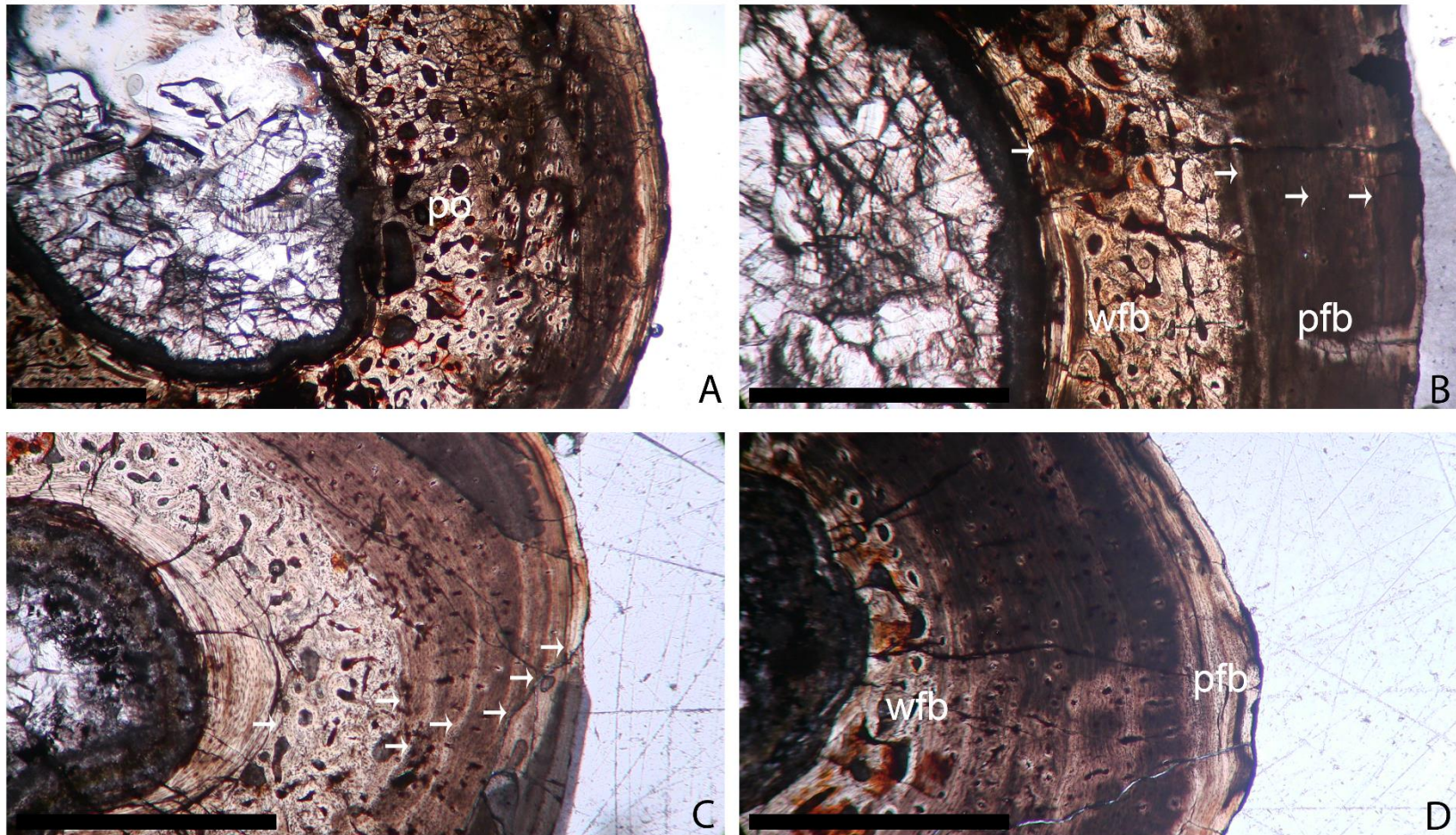


**Figure 7:** Histologic sections of limb bones. **A-B**, NCSM 16441 (fibula); **C-D**, NCSM 19765 (tibia). White arrows denote LAGs. pfb = parallel fibred bone; po = primary osteon; wfb = woven fibred bone. All scale bars 1 mm.

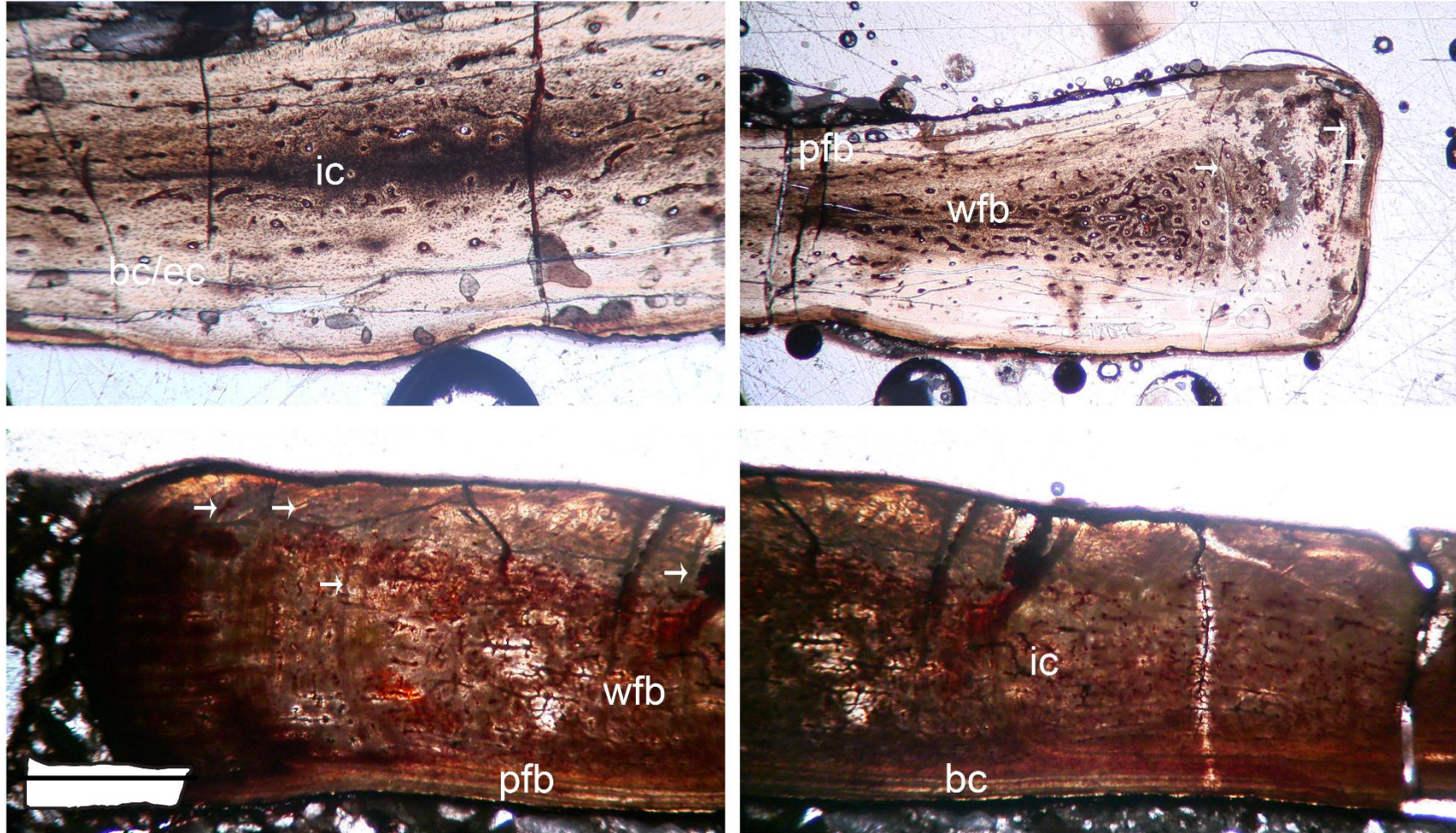


**Figure 8:** Transverse osteoderm sections. **A-B**, NCSM 18819A (lateral osteoderm); **C-D**, NCSM 20827 (paramedian osteoderm).

White arrows denote LAGs. bc = basal cortex; ec = external cortex; ic = internal core; pfb = parallel fibred bone; wfb = woven fibred bone. All scale bars 1 mm.

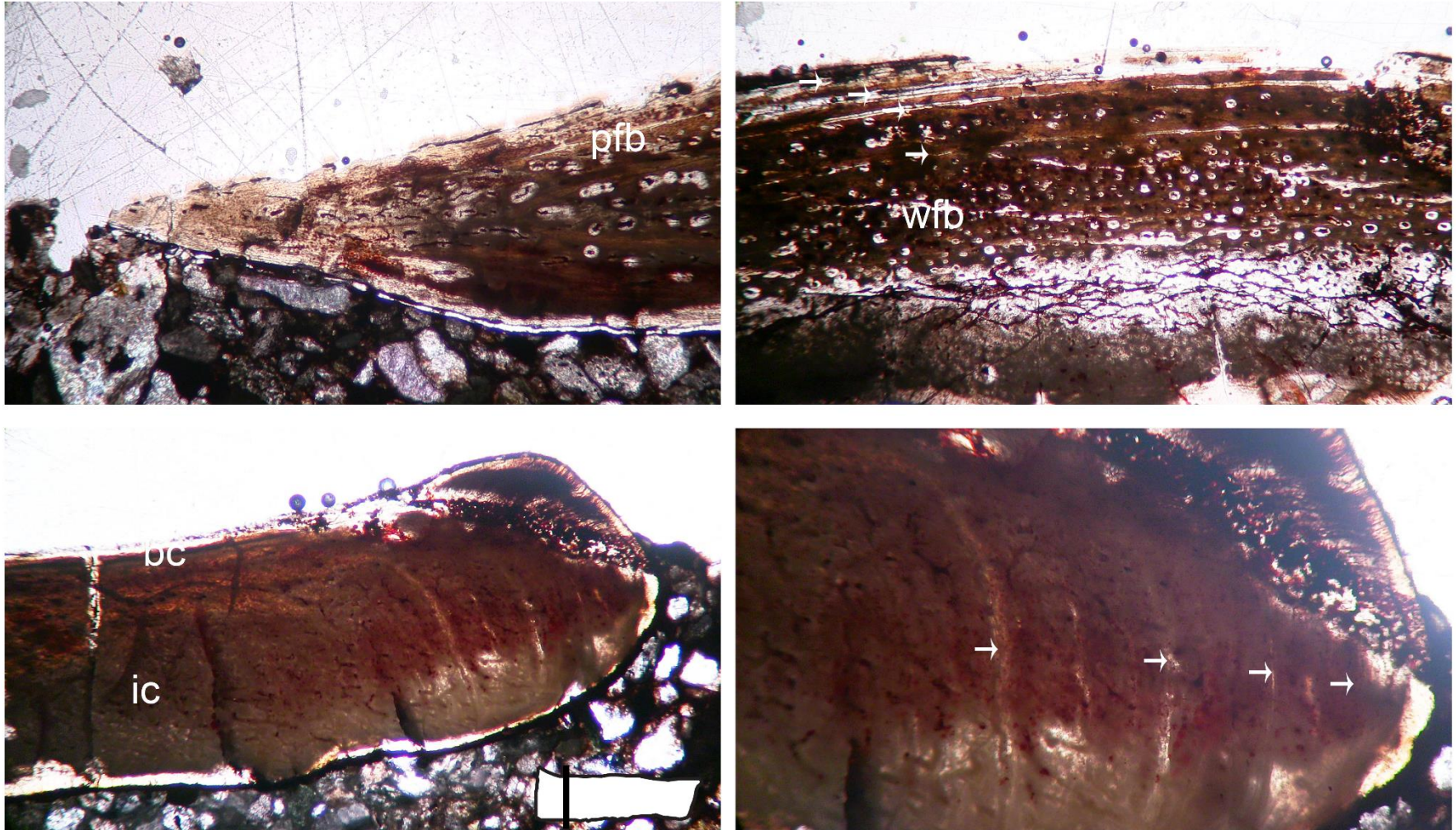


**Figure 9:** Parasagittal osteoderm sections. **A-B**, NCSM 21175 (paramedian(?) osteoderm); **C-D**, NCSM 26204 (paramedian osteoderm). White arrows denote LAGs. bc = basal cortex; ic = internal core; pfb = parallel fibred bone; wfb = woven fibred bone. All scale bars 1 mm.

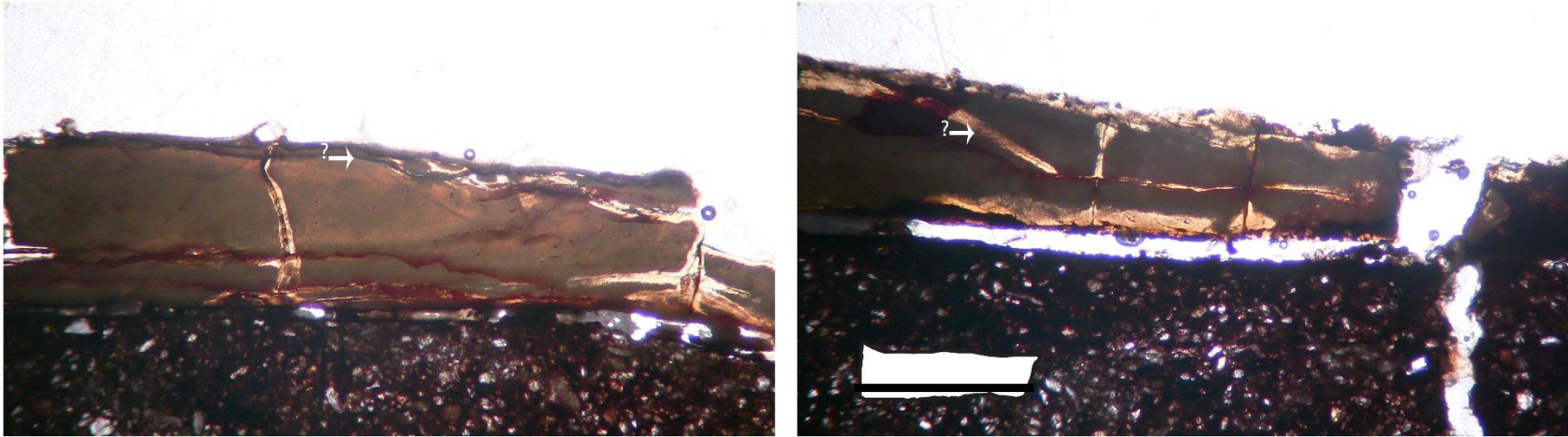


**Figure 10:** Type specimen (NCSM 23618) paramedian osteoderm posterior margin. White arrows denote uncertain LAGs. All scale bars 1 mm.